

Temperature-induced changes in the magnetism of Laves phase rare-earth–iron intermetallics by *ab initio* calculations

O. Šipr,^{1,2,*} S. Mankovsky,³ J. Vackář,⁴ H. Ebert,³ and A. Marmodoro^{1,†}

¹FZU – Institute of Physics of the Czech Academy of Sciences, Cukrovarnická 10, CZ-162 53 Prague, Czechia

²New Technologies Research Centre, University of West Bohemia, CZ-301 00 Pilsen, Czechia

³Department of Chemistry, Ludwig-Maximilians-Universität München, Butenandtstr. 11, D-81377 München, Germany

⁴FZU – Institute of Physics of the Czech Academy of Sciences, Na Slovance 2, CZ-182 21 Prague, Czechia

(Dated: August 10, 2022)

Laves RFe₂ compounds, where R is a rare earth, exhibit technologically relevant properties associated with the interplay between their lattice geometry and magnetism. We apply *ab initio* calculations to explore how magnetic properties of Fe in RFe₂ systems vary with temperature. We found that the ratio between the orbital magnetic moment μ_{orb} and the spin magnetic moment μ_{spin} increases with increasing temperature for YFe₂, GdFe₂, TbFe₂, DyFe₂, and HoFe₂. This increase is significant and it should be experimentally observable by means of x-ray magnetic circular dichroism. We conjecture that the predicted increase of the $\mu_{\text{orb}}/\mu_{\text{spin}}$ ratio with temperature is linked to the reduction of hybridization between same-spin-channel states of atoms with fluctuating magnetic moments and to the associated increase of their atomic-like character.

I. INTRODUCTION

Intermetallic C15-type Laves phase compounds RFe₂, where R is a rare earth, exhibit various properties linked to the interplay between magnetism and the crystal lattice [1]. One of them is a large or unusual magnetostrictive and magnetocaloric effect [2–4]. Another reason for interest comes from thermal or light induced magnetization switching studied intensively in doped amorphous Gd-Fe alloys with a composition close to GdFe₂ [5–7].

An essential part of the research on RFe₂ is exploring the various aspects how electronic states determine magnetism. An important goal is understanding the relation between orbital and spin contributions to the magnetic moments and how these contributions depend on parameters such as an external magnetic field or temperature. Recent interest in the relation between spin and orbital magnetism in situations when the system is not in the ground state [8] has been motivated, among other reasons, by efforts to understand the transfer between spin and orbital moments in ultrafast demagnetization [9–11] and by pursuits to comprehend the temperature-dependence of magnetocrystalline anisotropy [12].

Concerning the RFe₂ systems, most attention has been paid to the magnetic moments of the rare earth component so far. One of the reasons is that the experimental research aiming to separate the spin and orbital moments often employed techniques such as magnetic Compton scattering combined with vibrating sample or superconducting quantum interference device magnetometry [13–16], which are sensitive to the sums of rare-earth- and transition-metal-related contributions. As the moment of the rare earth is larger than the moment of Fe, the Fe contribution to magnetism of RFe₂ is often hidden

behind the contribution of the R atom. However, the intriguing properties of the RFe₂ compounds are significantly influenced also by the magnetism of the 3d element, because the interatomic interaction between the large 4f moments of the rare earth atoms depends on the exchange coupling mediated by the transition metal atoms.

Our aim is, therefore, to investigate magnetism of Fe in RFe₂. For practical applications as well as for fundamental insight it is important to understand how magnetic moments change due to finite temperature. We employ *ab initio* calculations to investigate how the spin magnetic moment μ_{spin} , the orbital magnetic moment μ_{orb} , and especially the ratio $\mu_{\text{orb}}/\mu_{\text{spin}}$ vary for RFe₂ if the temperature increases from zero to the Curie temperature T_C . To perform thermal averaging, we employ the alloy analogy model, which proved to be useful in studying the temperature-dependence of various magnetism-related properties in the past [17, 18]. We will show below that the $\mu_{\text{orb}}/\mu_{\text{spin}}$ ratio for Fe in RFe₂ increases with increasing temperature by as much as 70 %.

II. THEORETICAL SCHEME

The calculations were performed within the *ab-initio* framework of spin-density functional theory. A proper description of magnetism of rare earths requires special care for exchange and correlation effects due to the highly localized *f* electrons. We used the open core method in this work: the *f* electrons were treated as core electrons, with their numbers fixed during the self-consistency loop and with the spin and orbital moments set according to the *LS* coupling scheme [19, 20]. Despite its relative simplicity, many aspects of rare earths magnetism are described properly within this approach. Recently, this formalism was employed, e.g., to get parameters for the Landau-Lifshitz-Gilbert equation to describe heat-assisted magnetization switching in GdFe₂ and TbFe₂

* sipr@fzu.cz; <http://crysa.fzu.cz/ondra>

† marmodoro@fzu.cz

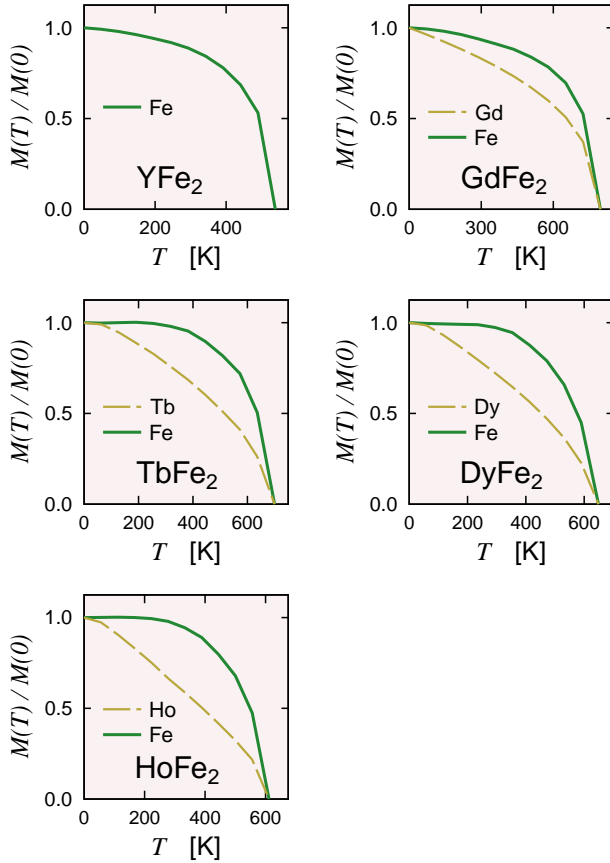


FIG. 1. Element-specific magnetization curves $M(T)$ used as input for our temperature-dependent calculations. Data for YFe_2 and GdFe_2 were taken from Morariu *et al.* [23], data for TbFe_2 , DyFe_2 , and HoFe_2 from Tang *et al.* [24].

[21]. Apart for the open core formalism for the f electrons, we relied on the local density approximation using the Vosko, Wilk, and Nusair functional [22].

The temperature effects were included by means of the alloy analogy model [17]: temperature-induced atomic displacements and spin fluctuations are treated as localized and uncorrelated, giving rise to disorder that can be described using the coherent potential approximation (CPA). Atomic vibrations were described using 14 displacement vectors. Each of the vectors was assigned the same probability and their amplitude was connected with the temperature by means of the Debye theory [17]. The Debye temperature was estimated as a weighted average of the Debye temperatures of elements constituting the RFe_2 compound.

Spin fluctuations were described by assuming that the local magnetic moments can get oriented along pre-defined directions; we sampled 60 values for the polar angle and 3 values for the azimuthal angle. The probability for each orientation was obtained by relying on the mean-field theory, using as an input the ratio of the

TABLE I. Magnetic moments for RFe_2 ($\text{R}=\text{Y, Gd, Tb, Dy, Ho}$) calculated for $T = 0$ K. The two top lines show moments for the R atom, then follow moments for the Fe atoms (for both symmetry-inequivalent sites if $\mathbf{M} \parallel [111]$), and the last two lines show total moments per formula unit.

		YFe_2	GdFe_2	TbFe_2	DyFe_2	HoFe_2
		$\mathbf{M} \parallel [111]$	$\mathbf{M} \parallel [111]$	$\mathbf{M} \parallel [111]$	$\mathbf{M} \parallel [001]$	$\mathbf{M} \parallel [001]$
μ_{spin}	R	0.499	7.732	6.670	5.622	4.580
μ_{orb}	R	-0.003	-0.026	2.977	4.979	5.981
μ_{spin}	Fe-1	-1.863	-2.004	-1.949	-1.919	-1.895
μ_{spin}	Fe-2	-1.864	-2.005	-1.951	—	—
μ_{orb}	Fe-1	-0.044	-0.061	-0.061	-0.055	-0.054
μ_{orb}	Fe-2	-0.053	-0.054	-0.053	—	—
μ_{spin}	tot	-3.228	3.722	2.769	1.784	0.790
μ_{orb}	tot	-0.104	-0.138	2.866	4.880	5.873

magnetization at the temperature T to the magnetization at $T = 0$, $M(T)/M(0)$ (see Ref. 17 for more details). Note that the ratio $M(T)/M(0)$ is used just to set the probabilities for pre-defined orientations of the magnetic moments; the values of respective spin and orbital moments are determined selfconsistently by the electronic structure calculation itself. Our approach differs in this respect from the rigid spin approximation, where it is assumed that the magnitude of magnetic moments is always the same no matter what the tilt angle is.

We allowed for atomic-element-dependent magnetization curves $M(T)$ resulting in element-dependent spin orientation probabilities. The input data for $M(T)/M(0)$ used in this work are shown in Fig. 1.

The calculations were done in a fully relativistic mode using the spin-polarized multiple-scattering or Korringa-Kohn-Rostoker (KKR) Green function formalism [25] as implemented in the SPRKKR code [26]. The potentials were subject to the atomic sphere approximation (ASA). We verified that this is not a severe restriction by performing the zero-temperature calculations not only in the ASA mode but also in the full-potential mode; the difference in magnetic moments was always less than 5 %. The energy integrals were evaluated by a contour integration on a semicircular path within the complex energy plane, using a Gaussian-Legendre quadrature on a mesh of 32 points. The \mathbf{k} -space integration was carried out via sampling on a regular mesh, making use of the symmetry, on a grid of $30 \times 30 \times 30$ points in the full Brillouin zone. For the multipole expansion of the Green function for valence electrons, the angular momentum cutoff $\ell_{\text{max}}=2$ was used.

III. RESULTS

A. Temperature-dependence of spin and orbital moments

Magnetic moments for RFe_2 ($\text{R}=\text{Y, Gd, Tb, Dy, Ho}$) calculated for zero temperature are presented in Tab. I. We show separately values of μ_{spin} and μ_{orb} for the rare earth and for Fe and also the total moments per formula unit. The signs are chosen so that the spin magnetic moment for the rare earth is positive. The magnetization direction \mathbf{M} is set either parallel to $[111]$ or to $[001]$, as indicated in the header. This setting was chosen in accordance with the easy axis of magnetization for each compound [27–29]. For GdFe_2 the situation is unclear [23, 27, 30], we have chosen $\mathbf{M}||[111]$.

If the magnetization is parallel to $[111]$, the spin orbit coupling reduces the symmetry of the system with respect to the case when there is no spin orbit coupling. This means that the four Fe sites which belong to the same type in the absence of spin orbit coupling are split into two types when it is included: the Fe-1 type comprises one site and the Fe-2 type comprises the other three sites. For $\mathbf{M}||[001]$ this symmetry reduction does not occur. The results presented in Tab. I are in a good agreement with earlier theoretical and experimental works for YFe_2 [31, 32], GdFe_2 [21, 33, 34], TbFe_2 [21, 28], DyFe_2 [28], and HoFe_2 [28, 35].

The calculated temperature-dependence of μ_{spin} , μ_{orb} , and $\mu_{\text{orb}}/\mu_{\text{spin}}$ for the Fe sites is shown in Fig. 2. We monitor two quantities, namely, (i) the magnitude of the magnetic moment and (ii) its projection on the easy axis of magnetization. These quantities were obtained by evaluating their configuration average by means of the alloy analogy model (Sec. II). We choose the notation $\langle|\mu|\rangle$ for the magnitude of the moment and $\langle\mu^{(z)}\rangle$ for its projection, with μ representing the magnetic moment (spin or orbital). By the superscript (z) we always mean the common magnetization direction (in our case, either $[111]$ or $[001]$).

Concerning the projections of the magnetic moments, one can observe by inspecting Fig. 2 that if the temperature increases, both $\langle\mu_{\text{spin}}^{(z)}\rangle$ and $\langle\mu_{\text{orb}}^{(z)}\rangle$ decrease so that they are zero at $T = T_C$, as mandated by the model. However, the situation differs for the magnitudes of the magnetic moments, where $\langle|\mu_{\text{spin}}|\rangle$ still decreases with increasing T but to a finite nonzero value at $T = T_C$, whereas $\langle|\mu_{\text{orb}}|\rangle$ increases with T . The fact that the local magnetic moments for Fe atoms are nonzero even at T_C resemble the behavior of Fe in other systems [36]. For the ratio $\mu_{\text{orb}}/\mu_{\text{spin}}$ it does not matter whether we evaluate the ratio of the projections $\langle\mu_{\text{orb}}^{(z)}\rangle/\langle\mu_{\text{spin}}^{(z)}\rangle$ or the ratio of the magnitudes $\langle|\mu_{\text{orb}}|\rangle/\langle|\mu_{\text{spin}}|\rangle$, both quantities increase with increasing T in the same way. This increase is by about 70 % in the interval from $T = 0$ K to $T = T_C$.

As mentioned in connection with Tab. I, there are two inequivalent Fe atomic types for $\mathbf{M}||[111]$. This distinc-

tion does not lead to apparent differences concerning the values of μ_{spin} but there are clear differences for μ_{orb} . If the temperature increases, these differences decrease (cf. the middle graphs in Fig. 2).

Further analysis shows that the temperature dependence of the magnetic moments is associated mainly with the fluctuations of the spin moments directions. Namely, additional calculations demonstrate that if the lattice vibrations are ignored, the results presented in Figs. 2 practically do not change (results not shown).

The electronic structure of the rare earth elements (Gd, Tb, Dy, Ho) is treated within the open core approach. The magnitude of the corresponding magnetic moments is thus temperature-independent and their projection on the common magnetization axis \mathbf{M} is just the average of the projections of the pre-defined spin directions weighted by corresponding thermodynamic probabilities (see Sec. II). In other words, the temperature dependence of the f electrons-related moments simply reproduces the respective input $M(T)$ curves shown in Fig. 1. As the f -electrons moments are dominant in rare earths, the same applies also to total spin and orbital moments of Gd, Tb, Dy, and Ho atoms. For this reason we do not show the curves here. Magnetism of Y in YFe_2 is induced by Fe and its temperature-dependence (not shown) therefore completely follows the temperature-dependence of the Fe moments.

B. Influence of a moment tilt on $\mu_{\text{orb}}/\mu_{\text{spin}}$

For further understanding, we examine what happens if the moment at a single Fe atom is gradually tilted with respect to the rest, taking GdFe_2 as an example. We assume that all magnetic moments are oriented along the same direction except for a single Fe atom, where the moment is tilted by the angle θ . The results for the magnitudes of spin and orbital moments and for their ratios are summarized in Fig. 3. One can see that the magnetic moment of a tilted Fe atom in GdFe_2 remains finite even for $\theta = 90^\circ$.

This provides another view on the $\mu_{\text{orb}}/\mu_{\text{spin}}$ ratio for the Fe atoms. Namely, the bottom graph of Fig. 3 shows that $\mu_{\text{orb}}/\mu_{\text{spin}}$ increases for Fe atoms with an increasing magnetization tilt angle. This is consistent with the increase of the $\mu_{\text{orb}}/\mu_{\text{spin}}$ ratio with increasing temperature demonstrated in Fig 2: within the alloy analogy model, larger temperature means bigger statistical weight of configurations with larger tilt angle (see Sec. II).

IV. DISCUSSION

We predict for several RFe_2 compounds that the ratio $\mu_{\text{orb}}/\mu_{\text{spin}}$ increases with increasing temperature. This prediction should be verifiable by x-ray magnetic circular dichroism (XMCD) experiments, because even though evaluating μ_{spin} and μ_{orb} separately by means of the

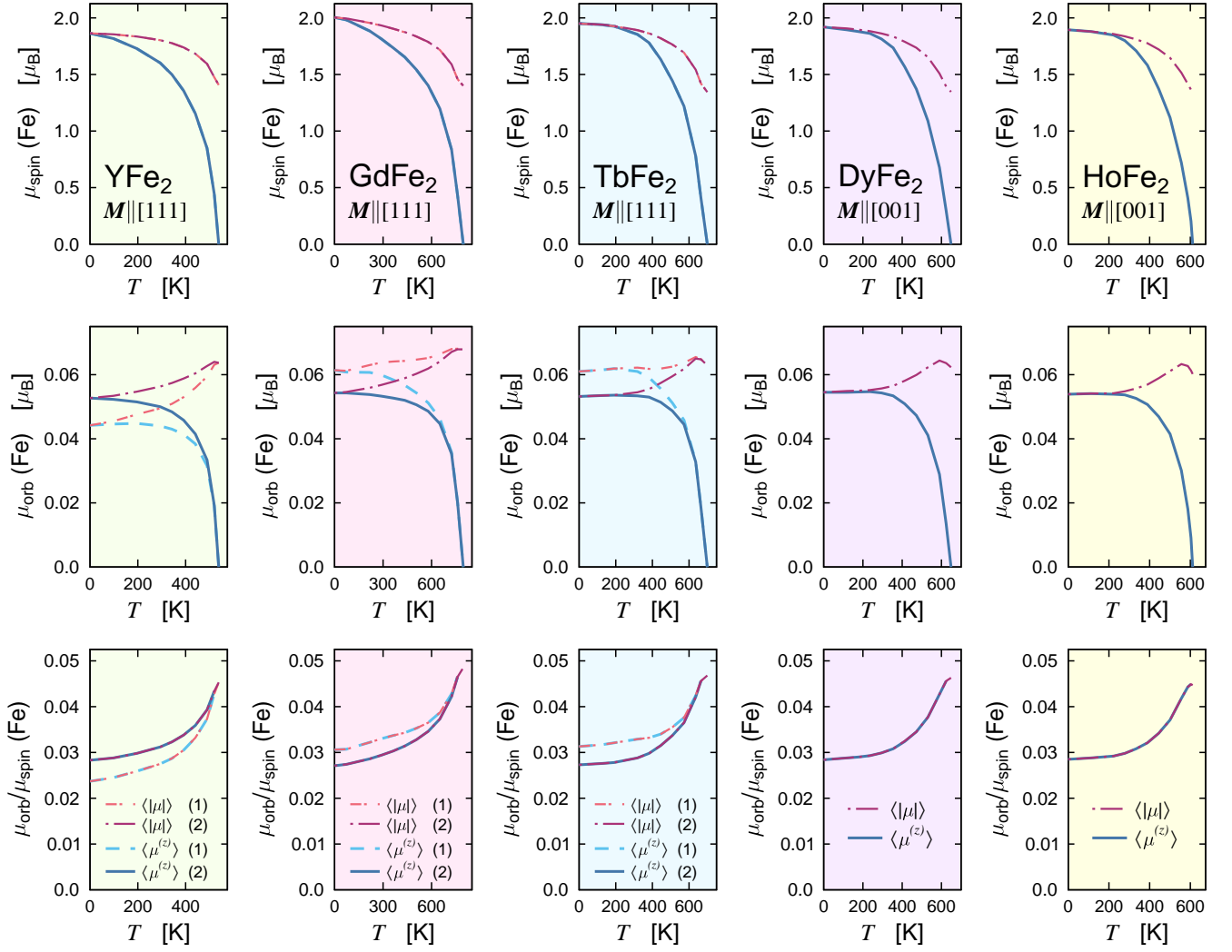


FIG. 2. Temperature-dependence of μ_{spin} (top graphs), μ_{orb} (middle graphs), and $\mu_{\text{orb}}/\mu_{\text{spin}}$ (bottom graphs) for Fe atoms in RFe_2 ($\text{R}=\text{Y}, \text{Gd}, \text{Tb}, \text{Dy}, \text{Ho}$). We present the magnitudes of the moments (curves labeled $\langle |\mu| \rangle$) and the projections of the moments on the common magnetization direction (curves labeled $\langle \mu^{(z)} \rangle$). The numbers (1) or (2) appearing in the legend for $\text{M} \parallel [111]$ distinguish between symmetry-inequivalent sites.

XMCD sum rules [37, 38] is not always straightforward, the determination of their ratio $\mu_{\text{orb}}/\mu_{\text{spin}}$ is much more robust and can serve as an indicator of even quite subtle effects [39]. In addition it should be noted that XMCD was already used for studying the temperature dependence of $\mu_{\text{orb}}/\mu_{\text{spin}}$ for Sm atoms in Laves compound $\text{Sm}_{0.974}\text{Gd}_{0.026}\text{Al}_2$ [40]. Analyzing corresponding data for Fe in RFe_2 systems would be more difficult because the magnetic moment of Fe is smaller than the magnetic moment of rare earth atoms and it further decreases for elevated temperatures where the increase of $\mu_{\text{orb}}/\mu_{\text{spin}}$ is to be observed. However, this should not be a severe problem. Our data indicate that for temperatures for which $\mu_{\text{orb}}/\mu_{\text{spin}}$ increases by 50 % with respect to $T = 0$ K, the magnetic moment for the Fe atoms de-

creases just to about half of its zero-temperature value (see Figs. 1–2). In such situation, an Fe $L_{2,3}$ -edge XMCD signal should be strong enough to be clearly resolved.

An intuitive explanation for the increase of $\mu_{\text{orb}}/\mu_{\text{spin}}$ with increasing temperature might be sought based on the lower graph of Fig. 3. Here we see that if the magnetic moment of a single Fe atom is tilted, the ratio $\mu_{\text{orb}}/\mu_{\text{spin}}$ increases; for the tilt angle $\theta = 90^\circ$ this increase is 20 %. Tilting the moment means reducing the hybridization between the states of the tilted atom and the states of surrounding atoms belonging to the same spin channel. In other words, the electron states associated with the tilted Fe atom become more atomic-like. In this limit, the experience shows that the $\mu_{\text{orb}}/\mu_{\text{spin}}$ ratio generally increases with respect to the bulk — compare,

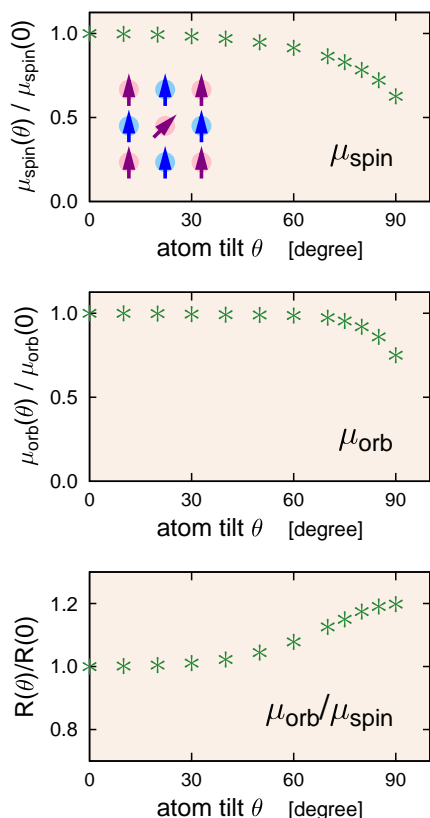


FIG. 3. Dependence of μ_{spin} , μ_{orb} , and the ratio $R=\mu_{\text{orb}}/\mu_{\text{spin}}$ for an Fe atom in GdFe_2 on the angle θ by which the moment for a single Fe atom is rotated. The quantities were evaluated for $T = 0$ K and normalized to their values at $\theta = 0^\circ$.

e.g., with the situation for clusters or surfaces [41, 42]. Increasing the temperature means increasing the statistical weights of atoms with tilted moments. We thus conjecture that the increase of $\mu_{\text{orb}}/\mu_{\text{spin}}$ with increasing temperature is linked to the reduction of the hybridization within the same spin channel between states of tilted Fe atoms. In this regard, one can see an analogy with the enhancement of μ_{orb} at surfaces: in that case the hybridization between the states of surface atoms is smaller than the hybridization between the states of bulk atoms. Analogously in our case, the hybridization between the states of atoms with tilted moments is smaller than the hybridization between the states of atoms with parallel

moments.

The increase of $\mu_{\text{orb}}/\mu_{\text{spin}}$ with increasing temperature appears to be quite a robust effect for RFe_2 systems. It occurs for any orientation of the magnetization and for any choice of R we considered. Note that R does not need to be a rare earth element — the effect occurs also for YFe_2 . One can expect that a similar effect, namely, temperature-related increase of the $\mu_{\text{orb}}/\mu_{\text{spin}}$ ratio, should occur for other systems as well. Prime candidates would be compounds with Fe atoms which have non-zero magnitude of the local magnetic moment even at temperatures close to T_C .

Let us now turn to the difference in μ_{orb} for symmetry-inequivalent Fe sites, as it happens for $\mathbf{M} \parallel [111]$ (see the graphs for YFe_2 , GdFe_2 , and TbFe_2 in Fig. 2). If the temperature approaches T_C , the difference between μ_{orb} at both sites gradually disappears. This is a consequence of the increased disorder in the spin directions when the temperature increases. At $T = T_C$ this disorder gets maximum, the magnetization direction \mathbf{M} ceases to have any meaning and the Fe sites become equivalent, similarly as they would be in the absence of spin-orbit coupling.

V. CONCLUSIONS

Ab-initio calculations with finite-temperature effects included by means of the alloy analogy model predict that the $\mu_{\text{orb}}/\mu_{\text{spin}}$ ratio increases with increasing temperature for RFe_2 Laves compounds. We interpret this as a consequence of reduced hybridization between states (within the same spin channel) of atoms with fluctuating spin magnetic moments and the associated increase of their atomic-like character if the temperature increases. The predicted enhancement of $\mu_{\text{orb}}/\mu_{\text{spin}}$ is large enough to be seen by XMCD experiments.

ACKNOWLEDGMENTS

This work was supported by the GA ĆR via the project 20-18725S. Additionally, computing resources were supported by the project CEDAMNF CZ.02.1.01/0.0/0.0/15_003/0000358, by the project “e-Infrastruktura CZ” (e-INFRA CZ LM2018140) and by the project “Information Technology for Innovation” (IT4I OPEN-22-42) provided by the Ministry of Education, Youth and Sport of the Czech Republic.

-
- [1] F. Stein, M. Palm, and G. Sauthoff, *Intermetallics* **12**, 713 (2004).
 - [2] A. Clark, in *Handbook of Ferromagnetic Materials*, Vol. 1, edited by E. P. Wohlfarth (Elsevier, 1980) pp. 531–589.
 - [3] V. Franco, J. Blázquez, J. Ipus, J. Law, L. Moreno-Ramírez, and A. Conde, *Prog. Mater. Sci.* **93**, 112

- (2018).
- [4] F. Stein and A. Leineweber, *J. Mater. Sci.* **56**, 5321 (2021).
- [5] I. Radu, K. Vahaplar, C. Stamm, T. Kachel, N. Pontius, H. A. Dürr, T. A. Ostler, J. Barker, R. F. L. Evans, R. W. Chantrell, A. Tsukamoto, A. Itoh, A. Kirilyuk,

- T. Rasing, and A. V. Kimel, *Nature* **472**, 205 (2011).
- [6] R. Chimata, L. Isaeva, K. Kádás, A. Bergman, B. Sanyal, J. H. Mentink, M. I. Katsnelson, T. Rasing, A. Kirilyuk, A. Kimel, O. Eriksson, and M. Pereiro, *Phys. Rev. B* **92**, 094411 (2015).
- [7] F. Jakobs, T. A. Ostler, C.-H. Lambert, Y. Yang, S. Salahuddin, R. B. Wilson, J. Gorchon, J. Bokor, and U. Atxitia, *Phys. Rev. B* **103**, 104422 (2021).
- [8] L. M. Sandratskii, *Journal of Physics: Condensed Matter* **26**, 426001 (2014).
- [9] E. Carpena, E. Mancini, C. Dallera, M. Brenna, E. Puppin, and S. De Silvestri, *Phys. Rev. B* **78**, 174422 (2008).
- [10] C. Boeglin, E. Beaurepaire, V. Halté, V. López-Flores, C. Stamm, N. Pontius, H. A. Dürr, and J.-Y. Bigot, *Nature* **465**, 458 (2010).
- [11] J. K. Dewhurst, S. Shallcross, P. Elliott, S. Eisebitt, C. v. K. Schmising, and S. Sharma, *Phys. Rev. B* **104**, 054438 (2021).
- [12] C. E. Patrick and J. B. Staunton, *Phys. Rev. Materials* **3**, 101401 (2019).
- [13] M. Itou, A. Koizumi, and Y. Sakurai, *Appl. Physics Lett.* **102**, 082403 (2013).
- [14] H. S. Mund, J. Sahariya, R. J. Choudhary, D. M. Phase, A. Dashora, M. Itou, Y. Sakurai, and B. L. Ahuja, *Appl. Physics Lett.* **102**, 232403 (2013).
- [15] B. Ahuja, H. Mund, J. Sahariya, A. Dashora, M. Halder, S. Yusuf, M. Itou, and Y. Sakurai, *J. Alloys Comp.* **633**, 430 (2015).
- [16] M. Yamazoe, T. Kato, K. Suzuki, M. Adachi, A. Shibayama, K. Hoshi, M. Itou, N. Tsuji, Y. Sakurai, and H. Sakurai, *J. Phys.: Condens. Matter* **28**, 436001 (2016).
- [17] H. Ebert, S. Mankovsky, K. Chadova, S. Polesya, J. Minár, and D. Ködderitzsch, *Phys. Rev. B* **91**, 165132 (2015).
- [18] O. Šipr, S. Wimmer, S. Mankovsky, and H. Ebert, *Phys. Rev. B* **101**, 085109 (2020).
- [19] M. Richter, in *Handbook of Magnetic Materials*, Vol. 13, edited by K. H. J. Buschow (North-Holland, Amsterdam, 2001) pp. 87–228.
- [20] O. Šipr, S. Mankovsky, and H. Ebert, *Phys. Rev. B* **100**, 024435 (2019).
- [21] R. Moreno, S. Khmelevskyi, and O. Chubykalo-Fesenko, *Phys. Rev. B* **99**, 184401 (2019).
- [22] S. H. Vosko, L. Wilk, and M. Nusair, *Can. J. Phys.* **58**, 1200 (1980).
- [23] M. Morariu, E. Burzo, and D. Barb, *J. Phys. Colloq.* **37 (C6)**, 615 (1976).
- [24] Y. Tang, X. Zhong, and H. Luo, *J. Magn. Magn. Materials* **127**, 378 (1993).
- [25] H. Ebert, D. Ködderitzsch, and J. Minár, *Rep. Prog. Phys.* **74**, 096501 (2011).
- [26] H. Ebert, *The SPRKKR package version 8*, <http://olymp.cup.uni-muenchen.de/ak/ebert/SPRKKR> (2018).
- [27] K. N. R. Taylor, *Adv. Phys.* **20**, 551 (1971).
- [28] A. Clark, R. Abbundi, and W. Gillmor, *IEEE Trans. Magn.* **14**, 542 (1978).
- [29] M. Budzynski, J. Sarzynski, M. Wiertel, and Z. Surowiec, *Nukleonika* **48 (suppl.1)**, S79 (2003).
- [30] U. Atzmony and M. P. Dariel, *Phys. Rev. B* **10**, 2060 (1974).
- [31] C. Ritter, *J. Phys.: Condens. Matter* **1**, 2765 (1989).
- [32] R. Sharma and Y. Sharma, *J. Supercond. Nov. Magn.* **90**, 1003 (2017).
- [33] S. Lee and K. Kim, *Solid State Commun.* **118**, 269 (2001).
- [34] S. M. Saini, N. Singh, T. Nautiyal, and S. Auluck, *J. Phys.: Condens. Matter* **19**, 176203 (2007).
- [35] G. E. Fish, J. J. Rhyne, S. G. Sankar, and W. E. Wallace, *J. Appl. Phys.* **50**, 2003 (1979).
- [36] A. V. Ruban, S. Khmelevskyi, P. Mohn, and B. Johansson, *Phys. Rev. B* **75**, 054402 (2007).
- [37] P. Carra, B. T. Thole, M. Altarelli, and X. Wang, *Phys. Rev. Lett.* **70**, 694 (1993).
- [38] B. T. Thole, P. Carra, F. Sette, and G. van der Laan, *Phys. Rev. Lett.* **68**, 1943 (1992).
- [39] O. Šipr, J. Minár, A. Scherz, H. Wende, and H. Ebert, *Phys. Rev. B* **84**, 115102 (2011).
- [40] S. S. Dhesi, G. van der Laan, P. Bencok, N. B. Brookes, R. M. Galéra, and P. Ohresser, *Phys. Rev. B* **82**, 180402 (2010).
- [41] O. Šipr, M. Košuth, and H. Ebert, *Phys. Rev. B* **70**, 174423 (2004).
- [42] V. Sessi, K. Kuhnke, J. Zhang, J. Honolka, K. Kern, C. Tieg, O. Šipr, J. Minár, and H. Ebert, *Phys. Rev. B* **82**, 184413 (2010).